Presymptomatic atrophy in autosomal dominant Alzheimer's disease: a serial MRI study

Authors:

Kirsi M. Kinnunen[a,1], David M. Cash[a,b,1], Teresa Poole[a,c], Chris Frost[a,c], Tammie L. S. Benzinger[d], R. Laila Ahsan[a], Kelvin K. Leung[a], M. Jorge Cardoso[a,b], Marc Modat[a,b], Ian B. Malone[a], John C. Morris[d], Randall J. Bateman[d], Daniel S. Marcus[d], Alison Goate[e], Stephen Salloway[f], Stephen Correia[f], Reisa A. Sperling[g], Jasmeer P. Chhatwal[g], Richard Mayeux[h], Adam M. Brickman[h], Ralph N. Martins[i], Martin R. Farlow[j], Bernardino Ghetti[j], Andrew J. Saykin[j], Clifford R. Jack Jr[k], Peter R. Schofield[l,m], Eric McDade[d], Michael W. Weiner[n], John M. Ringman[o], Paul M. Thompson[p], Colin L. Masters[q], Christopher C. Rowe[r], Martin N. Rossor[a], Sebastien Ourselin[a,b], Nick C. Fox[a]*, for the Dominantly Inherited Alzheimer Network (DIAN)

[1]*These authors contributed equally to this work*

[a]Dementia Research Centre, UCL Institute of Neurology, London, WC1N 3BG, UK, [b]Translational Imaging Group, UCL Centre for Medical Image Computing, London, NW1 2HE, UK, [c]London School of Hygiene & Tropical Medicine, WC1E 7HT, London, UK, [d]Departments of Radiology, Neurology, and Neurological Surgery & Psychiatry, Washington University School of Medicine, St. Louis, MO 63110, USA, [e]Department of Neuroscience, Icahn School of Medicine at Mount Sinai, New York, NY 10029-5674, USA, [f]Brown University-Butler Hospital, Providence, RI 02903, USA, [g]Department of Neurology, Massachusetts General Hospital, Harvard Medical School, Boston, MA 02114, USA, [h]Department of Neurology, Columbia University Medical Center, New York, NY 10032, USA, [i]School of Medical Sciences, Edith

Cowan University, Joondalup, WA 6027, Australia, [j]Departments of Neurology, Pathology and Laboratory Medicine and Radiology and Imaging Sciences, Indiana University School of Medicine, Indianapolis, IN 46202, USA, [k]Department of Radiology, Mayo Clinic, Rochester, MN 55905, USA, [l]Neuroscience Research Australia, Randwick NSW 2031, Australia, [m]School of Medical Sciences, University of New South Wales, Sydney, NSW 2052, Australia, [n]Department of Radiology, School of Medicine, University of California, San Francisco, CA 94143-0628, USA, [o]Department of Neurology, Keck USC School of Medicine, Los Angeles, CA 90089, USA, [p]Imaging Genetics Center, Keck School of Medicine, University of Southern California, Marina del Rey, CA 90292, USA, [q]The Florey Institute, The University of Melbourne, Heidelberg VIC 3084, Australia, [r]Department of Nuclear Medicine and Centre for PET and Department of Medicine, University of Melbourne, Austin Health, Heidelberg, VIC 3084, Australia

Corresponding author:

David M. Cash

Dementia Research Centre, UCL Institute of Neurology

Box 16, The National Hospital for Neurology and Neurosurgery

Queen Square

London WC1N 3BG

United Kingdom

Telephone: +44 203 448 3054

Fax: +44 (0)20 3448 3104

Email: d.cash@ucl.ac.uk

Abstract

INTRODUCTION: Identifying at what point atrophy rates first change in Alzheimer's disease is important for informing design of presymptomatic trials.

METHODS: Serial T1-weighed MRI scans of 94 participants (28 non-carriers, 66 carriers) from the Dominantly Inherited Alzheimer Network (DIAN) were used to measure brain, ventricular and hippocampal atrophy rates. For each structure, non-linear mixed effects models estimated the change-points when atrophy rates deviate from normal and the rates of change before and after this point.

RESULTS: Atrophy increased after the change-point, which occurred 1-1.5 years (assuming a single step change in atrophy rate) or 3-8 years (assuming gradual acceleration of atrophy) before expected symptom onset. At expected symptom onset, estimated atrophy rates were at least 3.6 times those before the change-point.

DISCUSSION: Atrophy rates are pathologically increased up to seven years before "expected onset". During this period, atrophy rates may be useful for inclusion and tracking of disease progression.

1. Background

Testing potentially disease-modifying treatments for Alzheimer's disease (AD) during the preclinical phase [1] presents challenges of recruitment and staging of asymptomatic individuals, as well as determining suitable measures for assessing disease modification. One recruitment strategy is to study members of families known to carry a pathogenic mutation in a gene – *presenilin 1 (PSEN1), presenilin 2 (PSEN2) or amyloid precursor protein (APP)* – that causes autosomal dominant AD (ADAD). These mutations have almost 100% penetrance and ~50% of at-risk individuals are carriers. ADAD typically has an early and relatively predictable age at symptom onset [2,3]. The Dominantly Inherited Alzheimer Network (DIAN) is a multicentre observational study of individuals at risk of, or affected by, ADAD. DIAN performs longitudinal assessments of imaging, fluid biomarkers, and cognitive function, which reflect pathological features in ADAD [4] and sporadic AD [5]. In particular, cerebral atrophy measures derived from volumetric magnetic resonance imaging (MRI) are used as biomarkers of neurodegeneration and as outcome measures in trials [6].

Longitudinal data from presymptomatic ADAD individuals provide a unique opportunity to determine when atrophy rates begin to diverge from normal. Previous cross-sectional, or small longitudinal studies report a wide range of estimates of this point of divergence: from 10 years before [4,7] to 7 years after [8] expected clinical onset (as determined by the affected parent's age at onset).

Abbreviations: DIAN = Dominantly Inherited Alzheimer Network; ADAD = autosomal dominantly inherited familial AD; PSEN1 = presenilin 1; PSEN2 = presenilin 2; APP = amyloid precursor protein; EAO = expected age at onset; EYO = estimated years to expected symptom onset; NC = mutation non-carriers; pMut+ = presymptomatic mutation carriers; qMut+ = questionably or mildly symptomatic mutation carriers; sMut+ = overtly symptomatic mutation carriers.

We used serial MRI data from DIAN to model cerebral atrophy rates during presymptomatic and early symptomatic stages of ADAD. We assessed whole brain and hippocampal atrophy and ventricular expansion, three well-established imaging measures used as exploratory endpoints in clinical trials [6]. We hypothesize that presymptomatic carriers have similar atrophy rates to non-carriers up until a 'change-point' when the biomarker starts to diverge from normal. This hypothesis is consistent with models of sporadic AD [5] that assume a sigmoidal trajectory, and cross-sectional findings from the DIAN cohort [4,7]. We used two non-linear mixed effects models (Supplementary Appendix A) to estimate the timing of change-points relative to expected symptom onset, and atrophy rates before and after these change-points. The first model assumes that the atrophy rate undergoes a single 'step change' to a new, stable value; whereas the second model assumes a 'gradual acceleration' in atrophy rate after the change-point. These models help characterize when therapeutic effects on brain atrophy could potentially be observed in presymptomatic ADAD and could help focus future sample size calculations for upcoming prevention trials.

2. Methods

2.1 Participants and Procedures

All participants were members of DIAN [9], and details of participating sites are available (http://dian-info.org/). The study received prior approval from appropriate Institutional Review Boards and Ethics Committees at each site. Informed consent was obtained from all participants.

Genotyping was performed to determine the presence of an ADAD mutation for each at-risk participant. A semi-structured interview assessed the expected age at onset (EAO), based on when the affected parent first showed progressive cognitive decline. Expected years to symptom onset (EYO) is the difference between age at scan and EAO [3]. Negative values indicate years before expected onset and positive values years after.

At the sixth data freeze (July 2013), there were 102 participants with two or more MRI scans available and complete data (mutation status, age, EAO, and global Clinical Dementia Rating (CDR) score [10]).

2.2 Volumetric MRI

Volumetric T1-weighted scans were acquired on 3 Tesla MRI scanners using Alzheimer's Disease Neuroimaging Initiative (ADNI) standardized protocols [11] and corrected for intensity inhomogeneity [12]. Whole brain and hippocampal regions were automatically segmented [13–15]. Lateral ventricles were delineated semi-automatically by an expert rater. Baseline volumetric measures were corrected for total intracranial volume (TIV), calculated using an automated technique [16]. For each structure, volume change was directly measured using a group-wise implementation [17–19] of the Boundary Shift Integral (BSI) [20] to ensure longitudinal consistency. A trained image analyst, blinded to participants' mutation and clinical status, reviewed all raw and processed images.

2.3 Clinical Classification

Participants were classified into four groups, based on mutation status, global CDR score, and actual age at onset (where this had occurred), determined by Uniform Data Set form B9, "Clinical Judgment of symptoms" [21]:

- **Mutation non-carriers (NC);** our control group.

- **Presymptomatic mutation carriers (pMut+)**; included mutation carriers with a global CDR score of 0 at both their first two visits.

- **Questionably or mildly symptomatic mutation carriers (qMut+);** included participants with at least one global CDR score of 0.5 during their first two visits, with the other visit being either 0 or 0.5. We excluded from this group participants who had a reported onset more than four years before study entry.

- **Overtly symptomatic mutation carriers (sMut+)**; included participants with a CDR score of 1.0 or greater at either (or both) of their first two visits or who were more than four years after reported onset at study entry.

Eight participants were excluded from the analysis: seven (one NC, four pMut+, one qMut+, one sMut+) were identified during initial visual review of the image data and excluded due to non-Alzheimer's pathology (e.g. infarct, neoplasm), imaging artifacts, or acquisition-related changes likely to result in unreliable atrophy measures. An additional participant (qMut+) was excluded due to moderate motion artefact on follow-up imaging and implausible growth in brain and hippocampi. As part of the sensitivity analysis, we re-ran the model including this participant (Supplementary Appendix B).

Two participants who initially satisfied the qMut+ criteria were retrospectively re-classified as sMut+, as both participants had consistent evidence of cognitive decline over a sustained period.

Our final sample therefore included 94 participants: 24 pMut+, 18 qMut+, 24 sMut+, and 28 NC. Of the 66 carriers, 54 had mutations in PSEN1, three in PSEN2, and nine in APP. There were 66 participants with two MR scans, 20 with three, and eight with four scans. The scan interval between baseline to follow-up ranged from 0.9 to 3.3 years, and was independent of carrier status or clinical severity. Two participants (one qMut+ and one sMut+) had inadequate image quality for analyses involving hippocampi.

2.4 Statistical analysis

To compare baseline values between each of the three mutations groups (pMut+, qMut+, sMut+) and the non-carrier group, ANOVA models were used for age, EYO, and TIV, while logistic regression was used for APOE $\varepsilon 4$ positivity and sex. A generalized least squares linear regression model that allows different group-specific residual variances was used to compare baseline volumes (standardized to mean TIV) between each of the three carrier groups and non-carriers.

The change-point model [22–24] was used to explore brain, ventricular and hippocampal atrophy rates (Supplementary Appendix A provides a detailed model description). As the focus of our study was the presymptomatic and earliest symptomatic stages of ADAD, the model included non-carriers (NC), presymptomatic, and questionably symptomatic carriers (pMut+/qMut+).

Figure 1 provides a schematic representation of the 'step change' and 'gradual acceleration' change-point models. In both, β represents the shared atrophy rate for NC and pMut+/qMut+ groups before the change-point, which takes place δ years before or after the EAO. Due to limited data, δ (for a specific brain structure) was assumed to be the same for all pMut+/qMut+ individuals.

For the 'step change' model, γ is the change in atrophy rate for the pMut+/qMut+ group after the change-point. In the 'gradual acceleration' model, the atrophy rate for the pMut+/qMut+ group accelerates after the change-point by a value of 2γ per year. With each model, we estimated β, γ and δ for each region, and using these we estimated atrophy rates at various points before and after EAO.

Our change-point model was not designed to estimate atrophy rates several years after symptom onset; to do so risked distorting a model that was designed to focus on the progression from early changes to clinical symptoms. Thus, a separate linear mixed-effects random-slopes model (with no change-point) was used to model atrophy rates of the sMut+ group, assuming all observations were after the change-point.

The change-point models are non-linear extensions of a previously described linear mixed-effects random-slopes model [25] (Supplementary Appendix A). Atrophy measures were log-transformed to provide symmetric approximations of percentage change from baseline. The change-point models were implemented using SAS

(version 9.4) procedure NLMIXED, which simultaneously estimated β, γ and δ. Robust estimates of uncertainty for these coefficients were obtained through bootstrapping [26,27], with 10,000 replicates and using bias corrected and accelerated (BCa) 95% confidence intervals. Sensitivity of the estimates and confidence intervals to outliers was explored (see Supplementary Appendix B).

3. Results

Table 1 summarizes demographic and clinical data. The sMut+ group was, as expected, older than the non-carriers, with smaller brain and hippocampal volumes, and larger ventricular volumes (all TIV-adjusted), reflecting pathological losses and larger TIV, which likely reflects the higher (albeit statistically non-significant) proportion of males in this group. The qMut+ group had smaller hippocampal volumes and larger ventricular volumes compared to non-carriers, while the preMut+ group just had smaller right hippocampal volumes.

Table 2 shows the change-point model results for each structure. In the 'step change' model, the pre-change atrophy rate (β) was statistically significant in every structure except the right hippocampus. In all regions, there were significant increases in atrophy rate (γ) after the change-point. This is demonstrated by deriving, from the results of the model, a ratio between the atrophy rate at EAO (1-0 years before) to the pre-change atrophy rate. This ratio was 4.0 for whole brain, 4.5 for ventricles, and 9.0 for left hippocampus, but it could not be produced for right hippocampus as the estimated pre-change atrophy rate was small and not statistically significantly different from zero. However, the increase in atrophy rate (γ) after the change-point for the right hippocampus was larger than the corresponding

coefficient in the results for the left hippocampus. The estimated change-point (δ) for brain, ventricle and left hippocampus was 1.4 years before EAO and 1.1 years before EAO for the right hippocampus. For whole brain and left hippocampus, the confidence intervals for δ did not span zero, providing evidence that they occurred before EAO. Estimates of the ventricular change-point had greater uncertainty (−1.1 to 13.5 years) than the other structures. Table 2 provides estimates for rates of change at various times before and after EAO.

As with the 'step change' model, in the 'gradual acceleration' model all structures except the right hippocampus had statistically significant pre-change atrophy rates. All regions had coefficients (γ) indicating statistically significant increased neurodegeneration after the change-point. The ratio of atrophy rate at EAO to the pre-change rate was 3.6 for whole brain, 4.1 for ventricles, and 5.1 for left hippocampus. The ratio for the right hippocampus was also not available due to the small, non-significant pre-change atrophy rate, but the coefficient (γ) indicated that the right hippocampus had a similar increase towards neurodegeneration as the left. The change-point estimates (δ) for the whole brain and ventricles were 3.0-4.6 years earlier than for the hippocampi. For all structures, the confidence intervals for δ did not span zero. Figure 2 shows estimated atrophy rates and 95% confidence intervals from both models in relation to EYO.

In the sensitivity analysis, we re-ran the model including the participant with movement artefact and clinically implausible data (Supplementary Appendix B). The pattern of the results was not materially altered although the statistical significance of some parameter estimates was lost.

The estimated rates of change in sMut+ participants were approximately double those found in pMut+/qMut+ carriers at EAO using the change-point models. The symptomatic rates were: −2.41% (95% CI: −2.88, −1.95) per year for whole brain, 15.0% (95% CI: 12.6,17.5) for ventricles, −4.70% (95% CI: −6.39, −3.01) for left hippocampus, and −4.64% (95% CI: −5.68, −3.60) for right hippocampus.

4. Discussion

The goal of this study was to estimate when brain, ventricular and hippocampal volume changes in ADAD diverge from non-carriers, and to model the rates before and after this transition using serial MRI data from the DIAN cohort. We designed two non-linear mixed effects models: one assuming a single 'step-change' and another assuming a 'gradual acceleration' in rates of atrophy after the change-point. This type of model has previously been used to investigate the trajectories of cognitive decline [23,28] and atrophy rates [29,30]. In all cases, there was evidence of increased atrophy after the change-point, suggesting that our models better reflect the non-linear nature of atrophy in early-stage disease than a linear relationship would. The 'gradual acceleration' model found evidence for all assessed regions that atrophy rates diverge from normal values before symptom onset, with the change-point occurring 3.0 to 7.6 years before EAO. The 'step change' model found a change-point of 1.4 years before EAO for whole brain and left hippocampus but was unable to show evidence of a change-point preceding EAO for ventricles or right hippocampus.

4.1 Interpreting the change-point model results

A key advantage of using two different change-point models is that they provide complementary information about the timing of the change-point. The 'step change' model provides the most conservative estimate of when atrophy rates diverge. In contrast, the 'gradual acceleration' model is probably more biologically plausible, based on previous results in ADAD [4,7,31,32] and by the well-characterised spatial spread of neurodegeneration [33] that typically begins in the medial temporal lobe and gradually spreads into neocortical regions. However, there are caveats to the gradual acceleration model used. The non-linear nature of the atrophy may vary between individuals and a quadratic may not be the most appropriate fit. However, given the size of the dataset, this approach minimizes risk of overfittings. Change-point models also avoid some of the pitfalls that can occur when including polynomial terms in a linear regression to model this non-linear relationship [34]. While a quadratic term could better capture the increase in atrophy rate observed around expected onset, it may also produce artefacts of increased atrophy in carriers who are decades before their expected onset.

Unlike linear models, change-point models can capture the different phases of atrophy/expansion during the long period of presymptomatic disease progression. Both models provide similar estimates of β (see Table 2), the pre-change atrophy rate. This suggested age-related changes broadly consistent with previous aging studies [35–37] showing small but significant rates of whole-brain atrophy of the order of 0.2-0.6%/year and hippocampal atrophy of the order of 0.3-0.4%/year for similar age ranges to this cohort. From both models, there was evidence of increased atrophy after the change-point in all regions.

4.2 Estimating onset of pathological atrophy

It is unclear when disease-related atrophy first becomes evident in ADAD. Cross-sectional results from *PSEN1* E280A mutation carriers [38,39] and DIAN [4,7] suggest atrophy of hippocampi diverge from non-carriers ~6 years and 10 years before symptom onset, respectively; earlier than in our models. However, initial longitudinal results from DIAN [7] (N=53) identified increased atrophy rates only in symptomatic carriers. A study of 13 presymptomatic *PSEN1* carriers found increased cortical thickness at baseline but subsequent thinning of a number of cortical regions [40], suggesting a non-linear nature to presymptomatic changes – with grey matter increases preceding declines.

Most previous longitudinal volumetric MRI studies of ADAD mutation carriers have been relatively small, single-site studies. One study following presymptomatic participants to clinical onset indicated pathological hippocampal atrophy rates appeared ~5.5 years before AD diagnosis [31]. Weston et al. [41] examined cortical thickness longitudinally in presymptomatic carriers and detected significant losses in the precuneus eight years before EAO. These values are consistent with our findings using a gradual acceleration model where the change point was 7.6 years before onset. However, another study of 16 ADAD mutation carriers (seven with long-term follow-up) did not detect structural MRI changes until *after* symptom onset [8], suggesting that a heterogeneity in these small cohorts and the methods used to analyze them may generate markedly different results.

No prior ADAD study has used change-point models, making it difficult to compare estimates. However, there are similarities between our findings and sporadic AD

studies that used similar approaches. A study of 79 elderly patients, 37 of whom developed mild cognitive impairment (MCI), reported a ventricular expansion change-point 2.3 years before MCI diagnosis [29]. Another longitudinal study (N=296, 66 progressing to MCI) found a similar hippocampal atrophy change-point of 2-4 years before clinical onset [30]. Their estimate of a 0.2% per year pre-change hippocampal atrophy rate accords with ours (0.2% left, 0.1% right). Their post-change atrophy rate estimate for the right hippocampus (2.7%/year) was similar to our value (2.5%) whereas their left hippocampal rate estimate (1.2%) was lower than our (2.1%).

4.3 Predicting clinical onset in ADAD

An important challenge is what estimate to use for clinical onset before it has occurred. Many studies, including ours, use an EAO based on when the affected parent first developed symptoms consistent with progressive decline. Other measures are based on the average across all previously affected family members, or the reported age at onset in the literature for a particular mutation [3]. However, each is an imperfect estimate of the future age at onset.

If future clinical trials use EYO as an inclusion criterion, then it is the distribution of atrophy rates relative to EAO that is of importance. However, if we wish to understand the etiology of the disease, then the distribution of atrophy rates relative to actual onset is more informative, as change-points are likely to be more strongly related to actual rather than expected age at onset. The effect of switching from actual to expected onset in statistical models will change the form of the estimated volume change over time, smoothing it to some degree. Without knowledge of actual

onset, this effect is not easily avoided. We did, however, attempt to reduce its impact by excluding overtly symptomatic carriers from our change-point models.

Identifying precisely when clinical onset has occurred is not straightforward. To facilitate standardization across sites, DIAN rigorously monitors how raters perform CDR and other assessments [42]. In at-risk individuals, other factors can influence cognitive function or behavioral changes, including stress, anxiety, and the constant level of vigilance and introspection that participants experience. In this study, there were six qMut+ participants who reverted from a baseline global CDR of 0.5 to 0 at follow-up. These cases highlight the subtle nature of transitions from unimpaired to "affected" and the potential confounds of mood disturbance and other factors. We addressed this uncertainty by including questionably or mildly symptomatic carriers in our change-point models.

4.4 Limitations and future work

Change-point models have been used to model atrophy rates in preclinical sporadic AD [29,30]. We expand on these approaches by adapting the model for repeated measures of direct change instead of individual volumetric measures and allowing for either a 'step change' or 'gradual acceleration' after the change-point. Due to the non-linear nature of our models, and the use of bootstrapping to obtain confidence intervals for the model coefficients, these models are susceptible to influential outliers, especially with smaller sample sizes (see the sensitivity analysis in Supplementary Appendix B). Additional longitudinal data should provide improved robustness against such issues.

No prior study has characterized the progression of atrophy in such a large cohort of presymptomatic and earliest symptomatic ADAD. DIAN is currently recruiting participants into a multicentre clinical trial [43], and the samples from our analysis should more closely reflect a clinical trial setting. Whole brain, lateral ventricles, and hippocampi are the most studied structures in sporadic AD, and are often used as trial outcome measures. From the results, these atrophy measures appear to be elevated compared to non-carriers approximately 5 years before expected onset, making them best suited for prevention trials in ADAD from this period onward. Given the evidence of presymptomatic atrophy in specific cortical regions [40,41], future application of the change-point model could involve studying atrophy rates of specific cortical structures, such as the precuneus and posterior cingulate. Atrophy in these structures may appear earlier and thus be better suited for trials that target presymptomatic patients. In addition, the model should incorporate information from other biomarkers, including CSF amyloid and tau concentrations, to determine how markers of these pathologies affect the timing of the change-point. Finally, it is essential to understand which preclinical changes in ADAD generalize to sporadic AD, as differences in the structures preferentially affected appear to exist [44].

4.5 Conclusions

Atrophy rates increase in ADAD some years before expected symptom onset. Using two different change-point models, we can characterize when this change occurs. The 'step-change' model provides a minimum estimate, 1.4 years before expected onset. The 'gradual acceleration' model provides a more biologically plausible approach towards how atrophy rates diverge from normal, with brain atrophy rates showing pathological acceleration ~7.6 years before expected onset and

hippocampal rates changing ~3.0 years before expected onset. These models may help predict the time to clinical onset for presymptomatic individuals with increased atrophy and identify individuals for prevention trials.

Figure captions

Figure 1: **Schematic representation of the 'step change' (Figure 1a) and 'gradual acceleration' (Figure 1b) change-point models.**

Figure 2: **Rates of change estimated from the 'step change' and 'gradual acceleration' models, as a function of the estimated years from symptom onset (EYO) for the pMut+/qMut+ carriers.**

The figure shows the relationship between rate of annualized volume change (%) and EYO. 95% confidence intervals are included, computed from the bootstrap samples. While the schematics in Figure 1 display the decline in actual volume, these graphs represent the rate of change in volume. A horizontal line indicates the estimated atrophy rate (from the 'step change' model) for non-carriers and carriers before the change-point before any deviation from normal rates of change. Vertical dotted lines indicate the change-points for both the 'step change' and 'gradual acceleration' models. For periods that include the change-point, the estimated rate of atrophy is a weighted combination representing the transition from the pre-change-point atrophy to the post-change-point atrophy. Top left: whole brain; top right: lateral ventricles; bottom left: left hippocampus; bottom right: right hippocampus.

Acknowledgements

References

[1]   Golde TE, Schneider LS, Koo EH. Anti-aβ therapeutics in Alzheimer's disease:
       the need for a paradigm shift. Neuron 2011;69:203–13.
       doi:10.1016/j.neuron.2011.01.002.

[2]   Ryan NS, Rossor MN. Correlating familial Alzheimer's disease gene mutations
       with clinical phenotype. Biomark Med 2010;4:99–112. doi:10.2217/bmm.09.92.

[3]   Ryman DC, Acosta-Baena N, Aisen PS, Bird T, Danek A, Fox NC, et al.
       Symptom onset in autosomal dominant Alzheimer disease: A systematic
       review and meta-analysis. Neurology 2014;83:253–60.
       doi:10.1212/WNL.0000000000000596.

[4]   Bateman RJ, Xiong C, Benzinger TLS, Fagan AM, Goate A, Fox NC, et al.
       Clinical and Biomarker Changes in Dominantly Inherited Alzheimer's Disease.
       N Engl J Med 2012;367:795–804. doi:10.1056/NEJMoa1202753.

[5]   Jack CR, Knopman DS, Jagust WJ, Petersen RC, Weiner MW, Aisen PS, et
       al. Tracking pathophysiological processes in Alzheimer's disease: an updated
       hypothetical model of dynamic biomarkers. Lancet Neurol 2013;12:207–16.
       doi:10.1016/S1474-4422(12)70291-0.

[6]   Cash DM, Rohrer JD, Ryan NS, Ourselin S, Fox NC. Imaging endpoints for
       clinical trials in Alzheimer's disease. Alzheimers Res Ther 2014;6:87.
       doi:10.1186/s13195-014-0087-9.

[7]   Benzinger TLS, Blazey T, Jack CR, Koeppe RA, Su Y, Xiong C, et al. Regional
       variability of imaging biomarkers in autosomal dominant Alzheimer's disease.
       Proc Natl Acad Sci U S A 2013;110:E4502-9. doi:10.1073/pnas.1317918110.

[8]   Yau W-YW, Tudorascu DL, McDade EM, Ikonomovic S, James JA, Minhas D,
       et al. Longitudinal assessment of neuroimaging and clinical markers in

autosomal dominant Alzheimer's disease: a prospective cohort study. Lancet Neurol 2015;14. doi:10.1016/S1474-4422(15)00135-0.

[9] Morris JC, Aisen PS, Bateman RJ, Benzinger TLS, Cairns NJ, Fagan AM, et al. Developing an international network for Alzheimer research: The Dominantly Inherited Alzheimer Network. Clin Investig (Lond) 2012;2:975–84. doi:10.4155/cli.12.93.

[10] Morris JC. The Clinical Dementia Rating (CDR): current version and scoring rules. Neurology 1993;43:2412–4.

[11] Jack CR, Bernstein MA, Borowski BJ, Gunter JL, Fox NC, Thompson PM, et al. Update on the magnetic resonance imaging core of the Alzheimer's disease neuroimaging initiative. Alzheimers Dement 2010;6:212–20. doi:10.1016/j.jalz.2010.03.004.

[12] Sled JG, Zijdenbos AP, Evans AC. A nonparametric method for automatic correction of intensity nonuniformity in MRI data. IEEE Trans Med Imaging 1998;17:87–97. doi:10.1109/42.668698.

[13] Leung KK, Barnes J, Modat M, Ridgway GR, Bartlett JW, Fox NC, et al. Brain MAPS: an automated, accurate and robust brain extraction technique using a template library. Neuroimage 2011;55:1091–108. doi:10.1016/j.neuroimage.2010.12.067.

[14] Cardoso MJ, Leung K, Modat M, Keihaninejad S, Cash DM, Barnes J, et al. STEPS: Similarity and Truth Estimation for Propagated Segmentations and its application to hippocampal segmentation and brain parcelation. Med Image Anal 2013;17:671–84. doi:10.1016/j.media.2013.02.006.

[15] Modat M, Ridgway GR, Taylor ZA, Lehmann M, Barnes J, Hawkes DJ, et al. Fast free-form deformation using graphics processing units. Comput Methods

Programs Biomed 2010;98:278–84. doi:10.1016/j.cmpb.2009.09.002.

[16] Malone IB, Leung KK, Clegg S, Barnes J, Whitwell JL, Ashburner J, et al. Accurate automatic estimation of total intracranial volume: a nuisance variable with less nuisance. Neuroimage 2014. doi:10.1016/j.neuroimage.2014.09.034.

[17] Leung KK, Ridgway GR, Ourselin S, Fox NC. Consistent multi-time-point brain atrophy estimation from the boundary shift integral. Neuroimage 2012;59:3995–4005. doi:10.1016/j.neuroimage.2011.10.068.

[18] Leung KK, Clarkson MJ, Bartlett JW, Clegg S, Jack CR, Weiner MW, et al. Robust atrophy rate measurement in Alzheimer's disease using multi-site serial MRI: Tissue-specific intensity normalization and parameter selection. Neuroimage 2010;50:516–23. doi:10.1016/j.neuroimage.2009.12.059.

[19] Leung KK, Barnes J, Ridgway GR, Bartlett JW, Clarkson MJ, Macdonald K, et al. Automated cross-sectional and longitudinal hippocampal volume measurement in mild cognitive impairment and Alzheimer's disease. Neuroimage 2010;51:1345–59. doi:10.1016/j.neuroimage.2010.03.018.

[20] Freeborough PA, Fox NC. The boundary shift integral: an accurate and robust measure of cerebral volume changes from registered repeat MRI. IEEE Trans Med Imaging 1997;16:623–9. doi:10.1109/42.640753.

[21] Morris JC, Weintraub S, Chui HC, Cummings J, DeCarli C, Ferris S, et al. The Uniform Data Set (UDS): Clinical and Cognitive Variables and Descriptive Data From Alzheimer Disease Centers. Alzheimer Dis Assoc Disord 2006;20:210–6. doi:10.1097/01.wad.0000213865.09806.92.

[22] Van Den Hout A, Muniz-Terrera G, Matthews FE. Smooth random change point models. Stat Med 2011;30:599–610. doi:10.1002/sim.4127.

[23] Hall CB, Lipton RB, Sliwinski M, Stewart WF. A change point model for

estimating the onset of cognitive decline in preclinical Alzheimer's disease.

Stat Med 2000;19:1555–66.

[24] Hall CB, Ying J, Kuo L, Lipton RB. Bayesian and profile likelihood change point methods for modeling cognitive function over time. Comput Stat Data Anal 2003;42:91–109. doi:10.1016/S0167-9473(02)00148-2.

[25] Frost C, Kenward MG, Fox NC. The analysis of repeated "direct" measures of change illustrated with an application in longitudinal imaging. Stat Med 2004;23:3275–86. doi:10.1002/sim.1909.

[26] Hyslop T. SAS macros for bootstrap samples with stratification and multiple observations per subject., 1995, p. 805–12.

[27] Barker N. A Practical Introduction to the Bootstrap Using the SAS System, 2005.

[28] Van Den Hout A, Muniz-Terrera G, Matthews FE. Change point models for cognitive tests using semi-parametric maximum likelihood. Comput Stat Data Anal 2013;57:684–98. doi:10.1016/j.csda.2012.07.024.

[29] Carlson NE, Moore MM, Dame A, Howieson D, Silbert LC, Quinn JF, et al. Trajectories of brain loss in aging and the development of cognitive impairment. Neurology 2008;70:828–33. doi:10.1212/01.wnl.0000280577.43413.d9.

[30] Younes L, Albert M, Miller MI. Inferring changepoint times of medial temporal lobe morphometric change in preclinical Alzheimer's disease. NeuroImage Clin 2014;5:178–87. doi:10.1016/j.nicl.2014.04.009.

[31] Ridha BH, Barnes J, Bartlett JW, Godbolt A, Pepple T, Rossor MN, et al. Tracking atrophy progression in familial Alzheimer's disease: a serial MRI study. Lancet Neurol 2006;5:828–34. doi:10.1016/S1474-4422(06)70550-6.

[32] Knight WD, Kim LG, Douiri A, Frost C, Rossor MN, Fox NC. Acceleration of cortical thinning in familial Alzheimer's disease. Neurobiol Aging 2011;32:1765–73. doi:10.1016/j.neurobiolaging.2009.11.013.

[33] Braak H, Braak E. Neuropathological stageing of Alzheimer-related changes. Acta Neuropathol 1991;82:239–59. doi:10.1007/BF00308809.

[34] Fjell AM, Walhovd KB, Westlye LT, Østby Y, Tamnes CK, Jernigan TL, et al. When does brain aging accelerate? Dangers of quadratic fits in cross-sectional studies. Neuroimage 2010;50:1376–83. doi:10.1016/j.neuroimage.2010.01.061.

[35] Allen JS, Bruss J, Brown CK, Damasio H. Normal neuroanatomical variation due to age: The major lobes and a parcellation of the temporal region. Neurobiol Aging 2005;26:1245–60. doi:10.1016/j.neurobiolaging.2005.05.023.

[36] Fraser MA, Shaw ME, Cherbuin N. A systematic review and meta-analysis of longitudinal hippocampal atrophy in healthy human ageing. Neuroimage 2015;112:364–74. doi:10.1016/j.neuroimage.2015.03.035.

[37] Walhovd KB, Westlye LT, Amlien I, Espeseth T, Reinvang I, Raz N, et al. Consistent neuroanatomical age-related volume differences across multiple samples. Neurobiol Aging 2011;32:916–32. doi:10.1016/j.neurobiolaging.2009.05.013.

[38] Quiroz YT, Stern CE, Reiman EM, Brickhouse M, Ruiz A, Sperling RA, et al. Cortical atrophy in presymptomatic Alzheimer's disease presenilin 1 mutation carriers. J Neurol Neurosurg Psychiatry 2013;84:556–61. doi:10.1136/jnnp-2012-303299.

[39] Fleisher AS, Chen K, Quiroz YT, Jakimovich LJ, Gutierrez Gomez M, Langois CM, et al. Associations Between Biomarkers and Age in the Presenilin 1

E280A Autosomal Dominant Alzheimer Disease Kindred. JAMA Neurol 2015;72:316. doi:10.1001/jamaneurol.2014.3314.

[40] Sala-Llonch R, Lladó A, Fortea J, Bosch B, Antonell A, Balasa M, et al. Evolving brain structural changes in PSEN1 mutation carriers. Neurobiol Aging 2015;36:1261–70. doi:10.1016/j.neurobiolaging.2014.12.022.

[41] Weston PSJ, Nicholas JM, Lehmann M, Ryan NS, Liang Y, Macpherson K, et al. Presymptomatic cortical thinning in familial Alzheimer disease: A longitudinal MRI study. Neurology 2016;87:2050–7. doi:10.1212/WNL.0000000000003322.

[42] Storandt M, Balota DA, Aschenbrenner AJ, Morris JC. Clinical and psychological characteristics of the initial cohort of the Dominantly Inherited Alzheimer Network (DIAN). Neuropsychology 2014;28:19–29. doi:10.1037/neu0000030.

[43] Bateman RJ, Benzinger TL, Berry S, Clifford DB, Duggan C, Fagan AM, et al. The DIAN-TU Next Generation Alzheimer's prevention trial: Adaptive design and disease progression model. Alzheimer's Dement 2016:1–12. doi:10.1016/j.jalz.2016.07.005.

[44] Cash DM, Ridgway GR, Liang Y, Ryan NS, Kinnunen KM, Yeatman T, et al. The pattern of atrophy in familial Alzheimer disease: volumetric MRI results from the DIAN study. Neurology 2013;81:1425–33. doi:10.1212/WNL.0b013e3182a841c6.

Table 1

Baseline demographics and region volumes for participants included in the longitudinal analysis.

	Non-carriers (NC)	Presymptomatic mutation carriers (preMut+)	Questionably or mildly symptomatic mutation carriers (qMut+)	Overtly symptomatic mutation carriers (sMut+)
N	28	24	18	24
Age, yrs (SD)	41.0 (8.4)	37.7 (10.1)	39.1 (10.2)	48.6 (8.2)[§]
Sex, F/M	17/11	16/8	11/7	10/14
APOE status, No. (%)*	6/28 (21%)	7/24 (29%)	6/18 (33%)	7/24 (29%)
Expected years to onset (EYO), yrs (SD)[†]	−5.52 (8.62)	−8.05 (8.38)	−4.19 (5.76)	4.01 (6.46)[§]
TIV, ml (SD)	1374 (129)	1373 (142)	1416 (124)	1483 (164)[§]
Brain volume, ml[‡] (95% CI)	1178 (1163, 1194)	1182 (1162, 1201)	1163 (1142, 1184)	1055[§] (1028, 1081)
Ventricular volume, ml[‡] (95%CI)	15.2 (13.0, 17.46)	15.4 (12.5, 18.3)	20.0[§] (15.9, 24.0)	34.3[§] (28.5, 40.1)
Left hippocampal volume, ml[‡] (95% CI)	3.01 (2.91, 3.10)	2.90 (2.79, 3.00)	2.73[§] (2.62, 2.84)	2.45[§] (2.28, 2.61)
Right hippocampal volume, ml[‡] (95% CI)	3.08 (2.99, 3.17)	2.93[§] (2.82, 3.01)	2.76[§] (2.63, 2.89)	2.55[§] (2.37, 2.73)

*Number (%) with APOE genotype 24, 34 or 44. [†]A negative value of EYO indicates that a participant joined the study before their expected age of onset, based on parental age at onset; EYO values for non-carriers are only indicative; EYO values

for overtly symptomatic mutation carriers do not reflect clinically determined actual age of onset. ‡Regional volumes were standardized to the mean TIV using a linear regression model. §$p < 0.05$ vs. NC.

Table 2a

Rates of change in whole brain and ventricular atrophy measures estimated using the step change and gradual

acceleration change-point models.

		Whole brain		Lateral ventricles	
		Step change	**Gradual acceleration**	**Step change**	**Gradual acceleration**
Annualized rate of pre-change atrophy (95% CI)		−0.28% (−0.42, −0.18)	−0.25% (−0.37, −0.11)	1.79% (0.44, 3.58)	1.59% (0.53, 2.91)
Post-change coefficient* (95% CI)		−0.84% (−1.22, −0.32)	−0.05 (−0.11, −0.01)	6.29% (1.99, 9.18)	0.45 (0.16, 1.17)
Change-point years before onset (95% CI)		1.4 (0.5, 3.8)	7.6 (2.3, 14.8)	1.4 (−1.1, 13.5)	6.0 (2.0, 15.5)
Atrophy rate (95% CI)	**10-9 years before**	−0.28% (−0.42, −0.18)	−0.25% (−0.39, −0.10)	1.79% (0.44, 3.58)	1.59% (0.44, 3.28)
	9-8 years before	−0.28% (−0.42, −0.18)	−0.25% (−0.38, −0.10)	1.79% (0.44, 3.58)	1.59% (0.43, 3.41)
	8-7 years before	−0.28% (−0.42, −0.18)	−0.26% (−0.38, −0.10)	1.79% (0.44, 3.58)	1.59% (0.43, 3.11)
	7-6 years before	−0.28% (−0.42, −0.18)	−0.35% (−0.66, −0.21)	1.79% (0.44, 3.58)	1.59% (0.26, 2.75)
	6-5 years before	−0.28% (−0.46, −0.18)	−0.44% (−0.77, −0.25)	1.79% (0.46, 3.60)	2.02% (0.64, 4.03)
	5-4 years before	−0.28% (−0.68, −0.18)	−0.53% (−0.86, −0.27)	1.79% (0.41, 3.57)	2.92% (1.20, 5.73)

4-3 years before	−0.28% (−0.79, −0.15)	−0.62% (−0.95, −0.30)	1.79% (0.30, 3.77)	3.82% (1.49, 6.57)
3-2 years before	−0.28% (−1.15, −0.14)	−0.72% (−1.04, −0.36)	1.79% (0.30, 4.18)	4.72% (2.00, 7.41)
2-1 years before	−0.64% (−1.21, −0.20)	−0.81% (−1.16, −0.48)	4.51% (1.82, 9.64)	5.62% (3.17, 8.34)
1-0 years before	−1.12% (−1.54, −0.66)	−0.90% (−1.27, −0.59)	8.07% (3.27, 15.24)	6.52% (4.34, 9.46)
0-1 years after	−1.12% (−1.52, −0.63)	−0.99% (−1.39, −0.64)	8.07% (3.00, 14.70)	7.42% (4.93, 10.53)
1-2 years after	−1.12% (−1.52, −0.64)	−1.09% (−1.53, −0.66)	8.07% (3.18, 10.90)	8.33% (5.39, 11.85)
2-3 years after	−1.12% (−1.52, −0.64)	−1.18% (−1.70, −0.67)	8.07% (3.50, 11.01)	9.23% (5.76, 13.66)

Table 2b

Rates of change in left and right hippocampal atrophy measures estimated using the step change and gradual acceleration change-point models.

		Left hippocampus		Right hippocampus	
		Step change	Gradual acceleration	Step change	Gradual acceleration
Annualized rate of pre-change atrophy (95% CI)		−0.23% (−0.44, −0.03)	−0.28% (−0.49, −0.07)	−0.07% (−0.24, 0.13)	−0.08% (−0.24, 0.13)
Post-change coefficient* (95% CI)		−1.82% (−3.28, −1.06)	−0.21 (−0.51, −0.12)	−2.42% (−6.45, −1.56)	−0.29 (−0.86, −0.15)
Change-point years before onset (95% CI)		1.4 (0.9, 1.8)	3.2 (2.0, 5.8)	1.1 (−2.0, 1.8)	3.0 (1.5, 6.2)
Atrophy rate	6-5 years before	−0.23% (−0.44, −0.03)	−0.28% (−0.51, −0.07)	−0.07% (−0.24, 0.13)	−0.08% (−0.25, 0.14)
	5-4 years before	−0.23% (−0.44, −0.03)	−0.28% (−0.58, −0.05)	−0.07% (−0.24, 0.13)	−0.08% (−0.28, 0.16)
	4-3 years before	−0.23% (−0.45, −0.03)	−0.28% (−0.65, 0.01)	−0.07% (−0.24, 0.13)	−0.08% (−0.30, 0.21)
	3-2 years before	−0.23% (−0.46, −0.03)	−0.57% (−1.36, −0.18)	−0.07% (−0.25, 0.13)	−0.39% (−1.19, −0.02)
	2-1 years before	−1.02% (−2.15, −0.19)	−0.99% (−1.82, −0.47)	−0.29% (−1.75, 0.20)	−0.98% (−1.75, −0.40)
	1-0 years before	−2.06% (−3.43, −1.28)	−1.42% (−2.40, −0.81)	−2.49% (−4.10, −1.79)	−1.57% (−2.37, −1.00)

0-1 years after	−2.06% (−3.52, −1.29)	−1.84% (−3.22, −1.14)	−2.49% (−4.85, −1.64)	−2.16% (−3.40, −1.45)
1-2 years after	−2.06% (−3.52, −1.29)	−2.27% (−4.19, −1.44)	−2.49% (−5.81, −1.64)	−2.74% (−4.80, −1.86)
2-3 years after	−2.06% (−3.52, −1.30)	−2.69% (−5.20, −1.74)	−2.49% (−6.74, −1.65)	−3.33% (−6.51, −2.23)

*For the 'step change' model, the post-change coefficient parameter o the model, γ, represents the change to the atrophy rate for presymptomatic and early symptomatic carriers after the change-point, and has units of percentage per year. In the 'gradual acceleration' model, the post-change coefficient is proportional to the rate of acceleration in the atrophy rate after the change-point. Due to this coefficient representing a time-squared term in the model, the rate of acceleration after the change point is a value of 2γ per year. This coefficient has units of percentage per year squared.
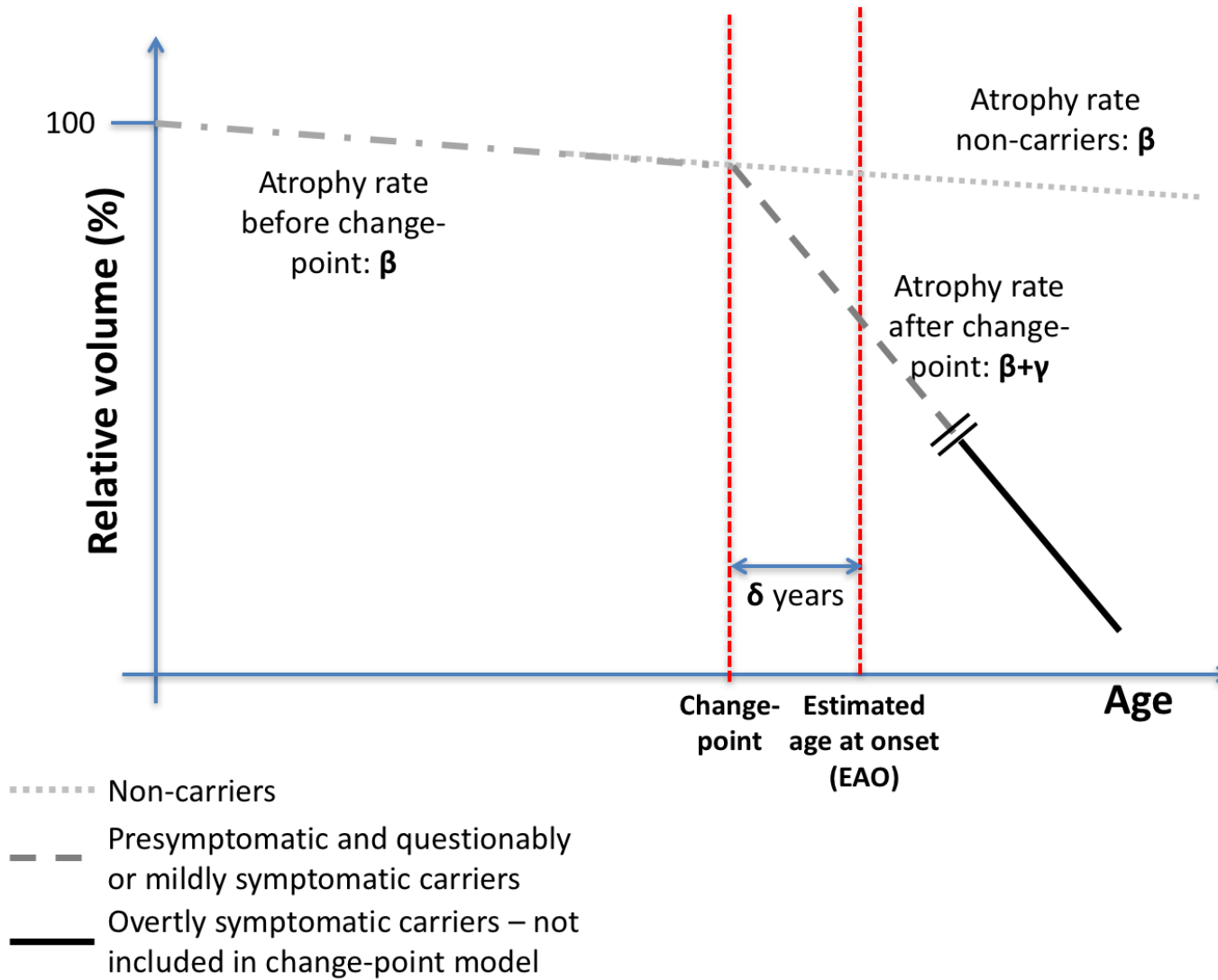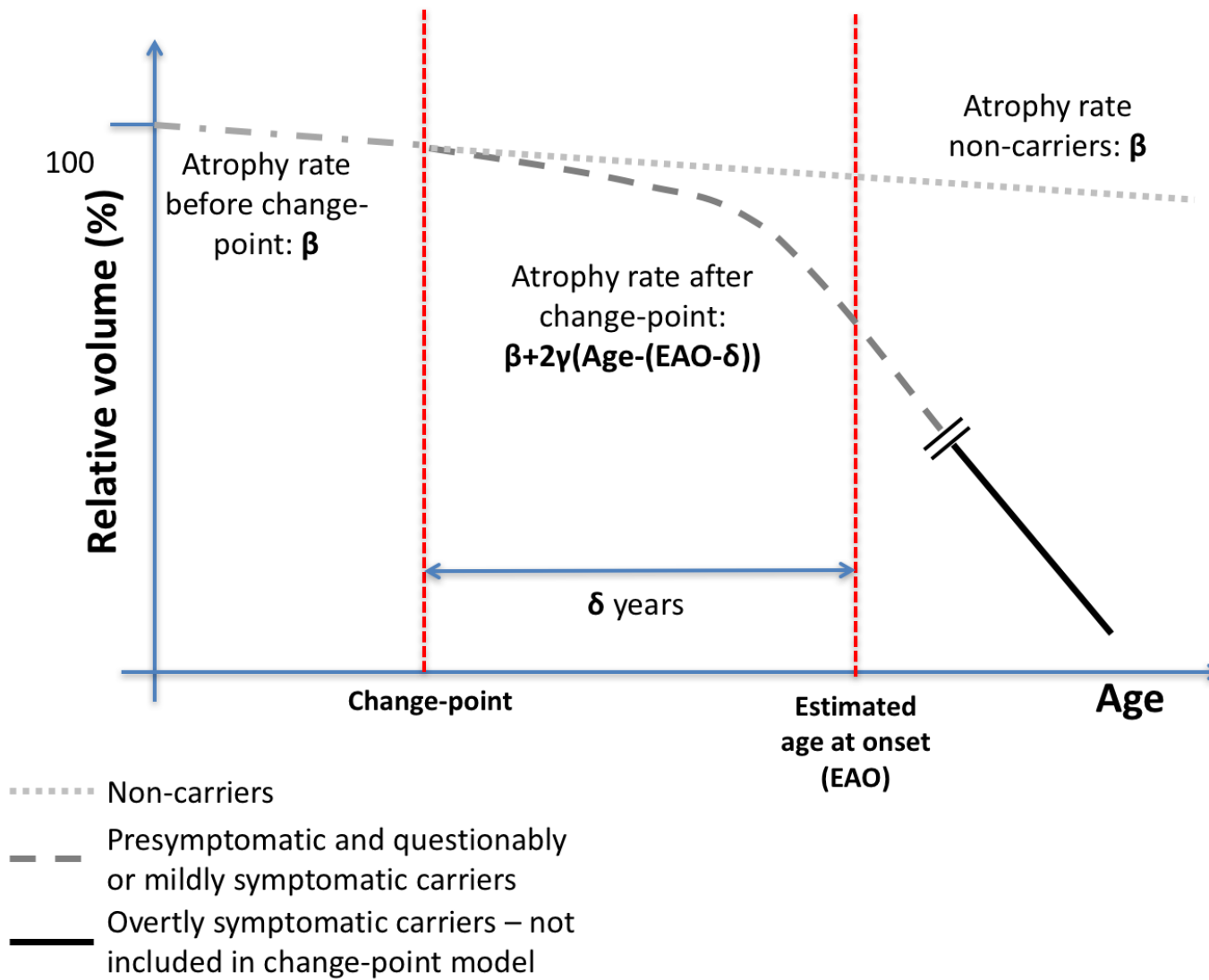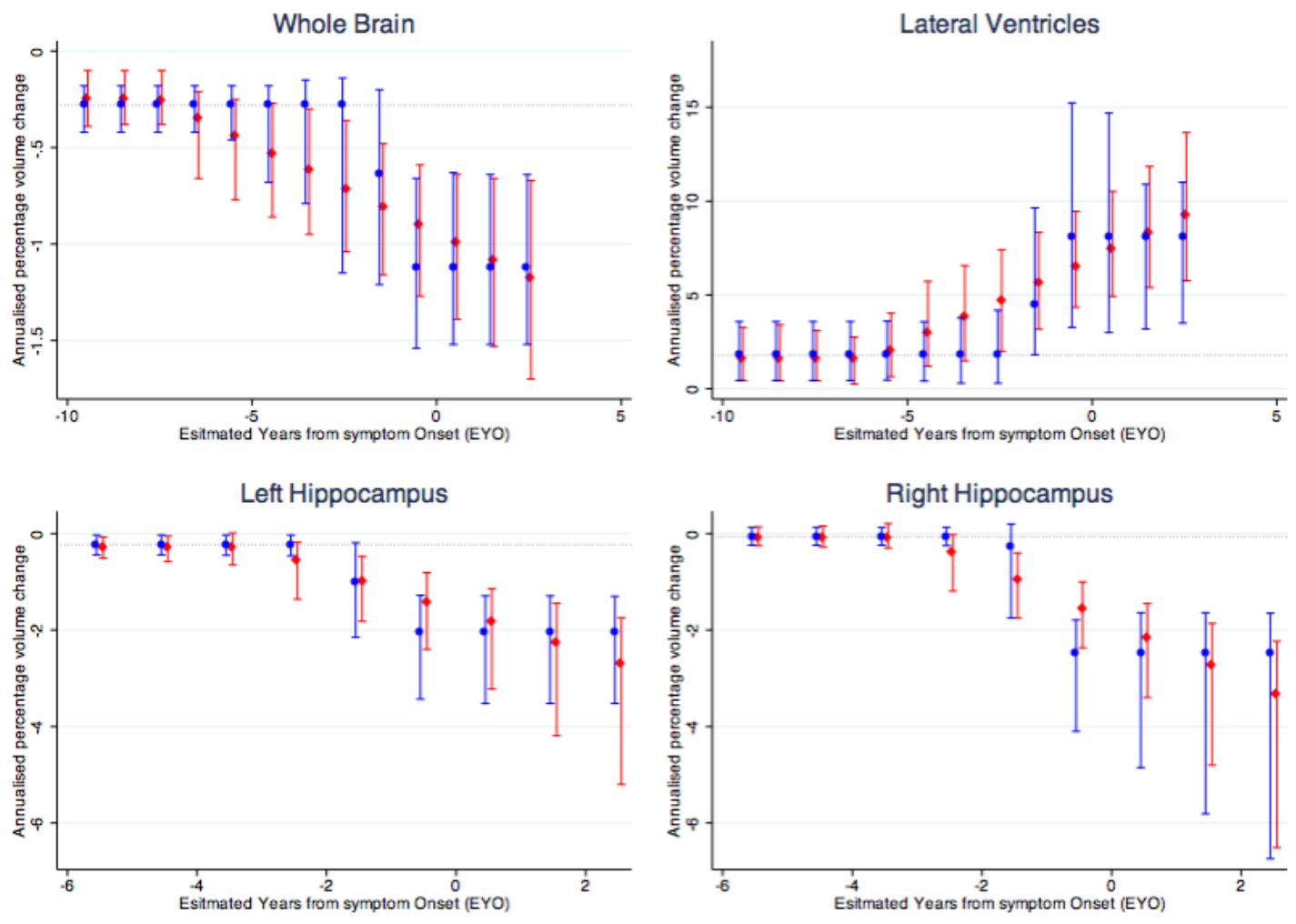
Figure 1(A)

Figure 1(B)

Figure 2

Supplementary Appendix A: Statistical methods and model development

The 'step change' version of the change-point model can be described by:

$$\log\left(\frac{Vol_{ij} + \Delta Vol_{ijk}}{Vol_{ij}}\right) = (\beta + b_i)(age_{ik} - age_{ij}) +$$
$$\gamma\left([age_{ik} - (EAO_i - \delta)]^+ - [age_{ij} - (EAO_i - \delta)]^+\right) + u_{ik} - u_{ij} + \eta_{ijk}$$

where, $X^+ = X$ if $X \geq 0$

(A.1)

$\quad\quad\quad = 0$ if $X < 0$

$\quad\quad\quad = 0$ for the NC group

and $b_i \sim N(0, \sigma_b^2)$; $u_{ij} \sim N(0, \sigma_u^2)$; $u_{ik} \sim N(0, \sigma_u^2)$; $\eta_{ijk} \sim N(0, \sigma_\eta^2)$.

Each observation for subject i includes measurements from two of the visits, the baseline visit (j) and one of the follow-up visits (k), at age_{ij} and age_{ik} respectively, with the measure of volume change between the two visits being the direct BSI measure ΔVol_{ijk}. All pairs of visits included the first (baseline) visit so there is only one choice of j but there is potentially more than one k (as some participants had more than two visits in total). In these models, $EYO_{ij} = age_{ij} - EAO_i$. The change-point terms X^+ allow only volume changes from pMut+/qMut+ participants with at least one scan visit within δ years of EAO to contribute to the estimation of γ. Individual variations in atrophy rate and between visits were included as random effects; b_i is the random subject specific deviation from the average atrophy rate (before the change-point); u_{ij} and u_{ik} are random subject specific deviations from the fixed effects at the baseline and follow-up visits respectively; η_{ijk} is the residual error. The 'gradual acceleration' version of the change-point model was obtained by squaring each of the X^+ terms.

$$\log\left(\frac{Vol_{ij} + \Delta Vol_{ijk}}{Vol_{ij}}\right) = (\beta + b_i)(age_{ik} - age_{ij}) +$$

$$\gamma\left(([age_{ik} - (EAO_i - \delta)]^+)^2 - \left([age_{ij} - (EAO_i - \delta)]^+\right)^2\right) + u_{ik} - u_{ij}$$

$$+ \eta_{ijk}$$

where, $X^+ = X$ if $X \geq 0$ (A.2)

$$= 0 \text{ if } X < 0$$

$$= 0 \text{ for the NC group}$$

and $b_i \sim N(0, \sigma_b^2)$; $u_{ij} \sim N(0, \sigma_u^2)$; $u_{ik} \sim N(0, \sigma_u^2)$; $\eta_{ijk} \sim N(0, \sigma_\eta^2)$.

During the development of the change-point models, we implemented the model in two different statistical packages: SAS and Stata (version 14.1), to check that we were getting consistent estimates from both. The results from the parallel Stata analyses for the 'step change' and 'gradual acceleration' change-point models were broadly consistent with the SAS results throughout, and have not been reported: they were subject to greater constraints than the SAS NLMIXED approach. In Stata, we used a 'two-stage' mixed effects modeling approach, where we first estimated δ, based on the profile likelihood, and then fixed this estimate for the model to determine β and γ, in line with an approach taken by many implementations of change point models [1-3]; confidence intervals for all parameters were obtained through bootstrapping.

Implementing the change-point models using SAS (version 9.4) procedure NLMIXED allowed us to estimate β, γ and δ in one process. The estimate of δ was restricted so that the change-point could not be later than two years after EAO; this was to ensure that a reasonable number of observations, at least 10, contributed to the estimation

of γ. When running the SAS analyses, the Nelder-Mead Simplex Optimization method was used, which does not require either first-order or second-order derivatives and does not assume that the objective function has continuous derivatives [4]. As non-linear models can be sensitive to parameter initialization [5], the parameter values for NLMIXED were initialized based on point estimates obtained from the parallel analyses using Stata. This initialization method also reduced computational time [6].

[1] Hall CB, Lipton RB, Sliwinski M, Stewart WF. A change point model for estimating the onset of cognitive decline in preclinical Alzheimer's disease. Stat Med 2000;19:1555–66.

[2] Carlson NE, Moore MM, Dame A, Howieson D, Silbert LC, Quinn JF, et al. Trajectories of brain loss in aging and the development of cognitive impairment. Neurology 2008;70:828–33. doi:10.1212/01.wnl.0000280577.43413.d9.

[3] Younes L, Albert M, Miller MI. Inferring changepoint times of medial temporal lobe morphometric change in preclinical Alzheimer's disease. NeuroImage Clin 2014;5:178–87. doi:10.1016/j.nicl.2014.04.009.

[4] NLMIXED Procedure, Optimization Algorithms. SAS/STAT(R) 9.22 User's Guide. Available at: https://support.sas.com/documentation/cdl/en/statug/63347/HTML/default/viewer.htm#statug_nlmixed_sect026.htm (last accessed 9 September 2016).

[5] Yao Q, Tong H. Quantifying the influence of initial values on nonlinear prediction. Journal of the Royal Statistical Society, Series B 1994; 56 (4): 701-725. ISSN 1369-7412.

[6] NLMIXED Procedure, Computational Problems. SAS/STAT(R) 9.2 User's Guide,

Second Edition. Available at:

https://support.sas.com/documentation/cdl/en/statug/63033/HTML/default/viewer.htm

#statug_nlmixed_sect032.htm (last accessed 9 September 2016).

Supplementary Appendix B: Sensitivity analysis

Sensitivity analysis was performed using the jackknife command in Stata. Each replicate of the jackknife removed all observations from a single participant: if they had only two time points and only one atrophy measurement, only one observation was removed. If they had more than two time points and thus multiple observations, all of these were removed in the jackknife replicate. Upon visual review of the scans and the measurements, for one participant there were biologically implausible measurements of change (large brain and hippocampal growth, shrinking ventricles) that appeared to be the result of movement in the follow-up scans compared to the baseline. When included in the sensitivity analysis, the resulting estimates from the jackknife replicate from this participant resulted in significantly modified estimates to the model compared to the rest of the replicates, indicating that it was acting as an influential point. This participant was removed from the dataset for the main analysis but we also repeated all of the analyses including this participant in order to investigate the sensitivity of the model design to an outlier. The following tables B.1 and B.2 are analogues of Tables 2(a) and (b) in the main paper for the analyses, but for analyses that include this participant.

We also performed some sensitivity analyses on the initialization of the parameters for the non-linear models. First we obtained profile plots of log likelihood with respect to a plausible range of parameter values to gain a sense of the smoothness of the optimization function with respect to the parameters, the approximate location of the global maximum, and the presence of any local maxima. Then we ran the model multiple times using different initialization settings. In all models, the results were relatively unchanged over a wide range of initial values for beta and gamma. The

parameter that was most sensitive to initialization was the delta parameter representing the change-point. Depending on the initial value for delta, the model appeared to reach different results for whole brain and ventricles in the step change model and for ventricles in the gradual acceleration model. In some cases, the estimate for delta deviated by 1-4 years from that obtained with the initialization settings used in the models that we report in the paper. However, in all cases, our initialization strategy – of basing the starting values on the results from the two-step approach in the Stata based model – resulted in obtaining the global (log likelihood) maximum. The different results obtained by perturbing the initialization values were due to the model becoming stuck in a local maximum. Our models' parameter estimates for left and right hippocampi did not appear sensitive to parameter initialization.

Supplementary Table B.1

Rates of change in whole brain and ventricular atrophy measures estimated using the step change and gradual acceleration change-point models including the participant with clinically implausible volume change data and motion artifact on followup imaging.

	Whole brain		Lateral Ventricles	
	Step Change	**Gradual Acceleration**	**Step Change**	**Gradual Acceleration**
Annualized rate pre-change-point (95% CI)	−0.28% (−0.43, −0.18)	−0.25% (−0.40, −0.13)	1.91% (0.32, 3.56)	1.67% (0.58, 3.05)
Post-change-point coefficient* (95% CI)	−0.68 (−1.10, −0.18)	−0.03 (−0.09, −0.01)	5.11 (−2.36, 8.21)	0.31 (−0.28, 0.82)
Change-point years before onset (95% CI)	1.6 (0.5, 4.1)	8.6 (3.2, 18.8)	1.4 (−1.2, 13.2)	7.2 (2.1, 19.8)

Supplementary Table B.2

Rates of change in left and right hippocampal atrophy measures estimated using step change and gradual acceleration change-point models including the participant with clinically implausible volume change data and motion artifact on followup imaging.

	Left hippocampus		Right hippocampus	
	Step Change	**Gradual Acceleration**	**Step Change**	**Gradual Acceleration**
Annualized rate pre-change-point (95% CI)	−0.22% (−0.43, −0.02)	−0.31% (−0.57, −0.11)	−0.09% (−0.28, 0.08)	−0.10% (−0.30, 0.10)
Post-change-point coefficient* (95% CI)	−1.49 (−2.56, −0.53)	−0.11 (−0.27, 0.60)	−1.86 (−3.14, −0.82)	−0.17 (−0.38, −0.02)
Change-point years before onset (95% CI)	1.8 (1.1, 2.4)	4.5 (2.3, 14.1)	1.4 (−0.1, 2.0)	4.3 (2.2, 13.0)

* For the 'step change' model, the post-change coefficient parameter o the model, γ, represents the change to the atrophy rate for presymptomatic and early symptomatic carriers after the change-point, and has units of percentage per year. In the 'gradual acceleration' model, the post-change coefficient is proportional to the rate of acceleration in the atrophy rate after the change-point. Due to this coefficient representing a time-squared term in the model, the rate of acceleration after the change point is a value of 2γ per year. This coefficient has units of percentage per year squared.